Gu et al., https://doi.org/10.1083/jcb.201606065

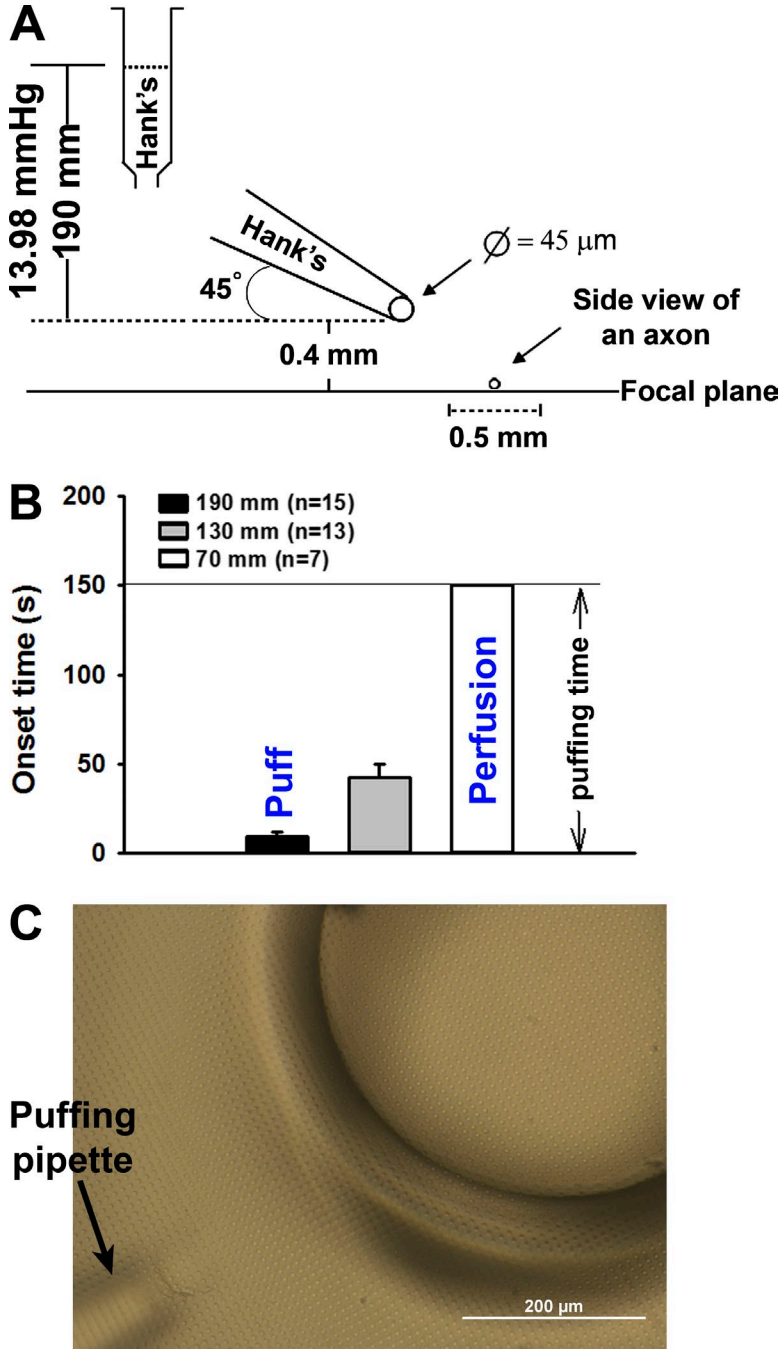

Figure S1. **The effect and strength of micromechanical pressure.** (A) Diagram of the puffing system. The glass pipette with tip diameter of ~45 µm is positioned at 45° angel and 0.4 mm above the focal plane. For puffing experiments, the buffer inside the pipette was always the same as the one in the bath. To provide puffing pressure, the tube connected with the puffing pipette was elevated 190 mm above its tip, providing ~13.98 mmHg static pressure at the pipette tip. For perfusion experiments, the tube was only elevated for 50 mm, under which no axonal varicosity was induced. The diameter of puffing areas is ~0.4 mm. (B) Axonal varicosity formation correlates with the strength of puffing in young axons (7 DIV). When the pressure was at 70 mmH_2O, no varicosity formation could be observed during 150-s puffing. Therefore, we used 50 mmH_2O for perfusion. Error bars indicate means ± SEM. (C) The membrane with arrays of microdots (4 µm in diameter and single spaced) received the same amount of fluid mechanical pressure as described in A. The field displacement reflected by the movement of microdots was determined by 3D microscope scanning and image processing and was used to calculate the pressure as described previously (Wang et al., 2013). Under our condition, the fluid mechanical force applied to neurons likely contained both shear and stretch partly because of the angel of puffing pipette. Moreover, it is important to note that the puffing pressure across the area was not uniform. Its center received a higher pressure than its peripheral regions, indicated by the biggest field displacement occurring at the center, where the mean pressure was measured in this study.

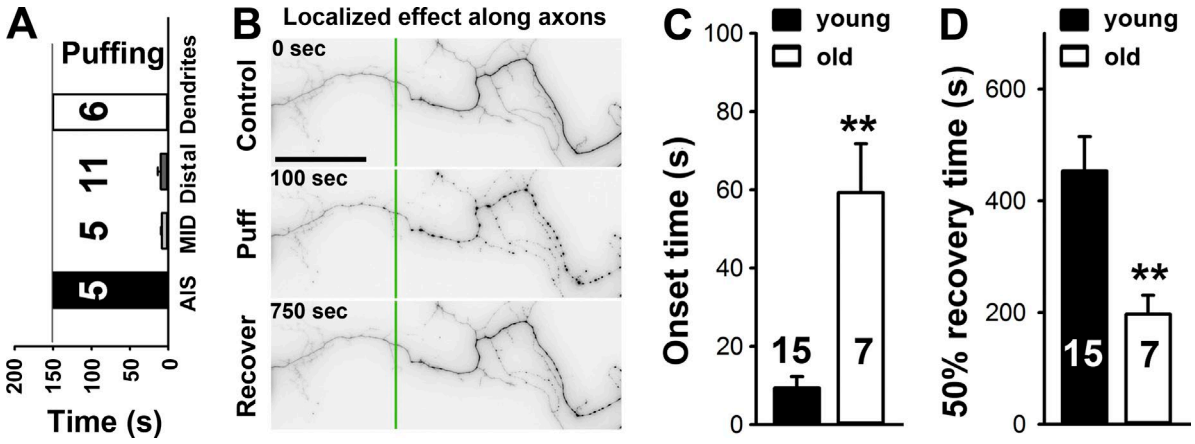

Figure S2. **Puffing-induced varicosity formation depends on the age and subcellular compartment of neurons.** (A) The onset time of puffing-induced varicosity formation in the AIS, middle (Mid), and distal axons as well as dendrites. Puffing lasted for 150 s. (B) Axonal varicosity initiation in response to puffing was highly localized. The borderline is indicated by green lines. Bars, 15 µm. (C and D) Under the same experimental condition, old (17 DIV) axons had markedly longer onset times (C) and shorter recovery times (D) compared with young axons (7 DIV) in Fig. 1 G. Error bars indicate means ± SEM. Unpaired *t* test: **, $P < 0.01$.

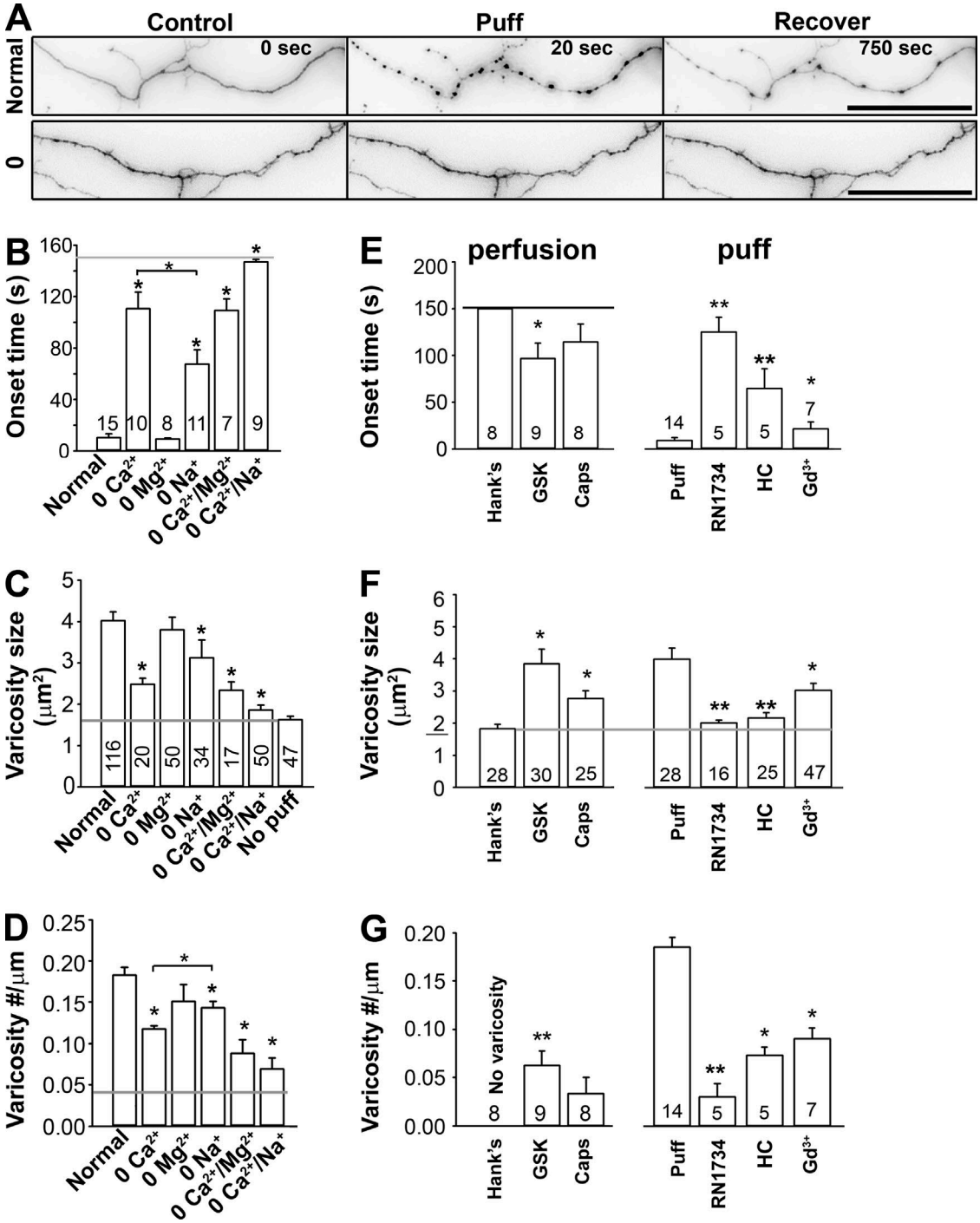

Figure S3. **Identification of MS ion channels responsible for puffing-induced varicosity formation in axons.** (A) Effects of puffing with normal Hank's buffer (top) or the buffer containing no Ca^{2+} and Na^{+} (bottom) on YFP-expressing axons. Bars, 20 μm. (B–D) Replacing different cations in the buffer had distinct effects on the onset time (B), the size (C; 2D area), and the density (D) of axonal varicosity formation in young neurons. (E–G) Summary of drug perfusion (left) and puffing (right) on the onset time (E), the size (F), and abundance (G) of axonal varicosities. Perfusion of 0.1 μM GSK101 (GSK; a TRPV4 agonist) but not 1 μM capsaicin (Caps; a TRPV1 agonist) markedly induced axonal varicosities. TRPV4-specific blockers RN1734 (10 μM) and HC067047 (HC; 100 nM) markedly inhibited puffing-induced axonal varicosity formation. A general inhibitor of MS ion channels (200 μM Gd^{3+}) also had some effect. All the experiments in this figure were performed on cultured hippocampal neurons at 7 DIV. Error bars indicate means ± SEM. Either a one-way ANOVA followed by Dunnett's test or an unpaired *t* test between Ca^{2+}-free and Na^{+}-free conditions was used. *, $P < 0.05$; **, $P < 0.01$.

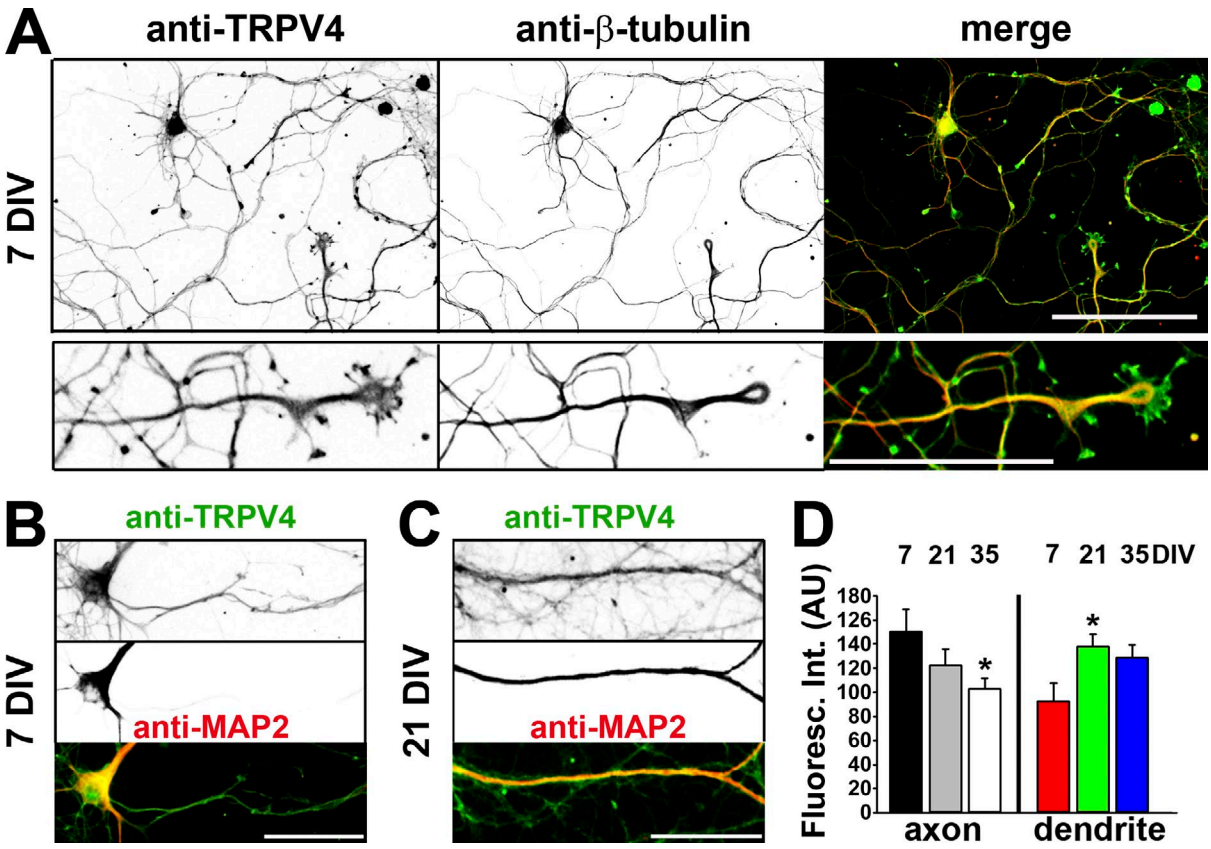

Figure S4. **TRPV4 expression in hippocampal neurons at different developmental stages.** (A) Costaining for endogenous TRPV4 (green in merged) and β-tubulin (red) in cultured hippocampal neurons at 7 DIV. Signals are inverted in grayscale images. Higher-magnification images are provided in bottom panels. (B and C) Young (7 DIV) and mature (21 DIV) neurons were costained for endogenous TRPV4 (green in merged) and MAP2 (red). Bars: (A, top) 100 µm; (A, bottom; B; and C) 40 µm. (D) Summary of fluorescence intensities of endogenous TRPV4 in axons (left) and dendrites (right) at different developmental stages. Mean fluorescence intensities in dendrites were measured between 10 µm away from the soma and the tip of the dendrite. n = ~20. Error bars indicate means ± SEM. One-way ANOVA followed by Dunnett's test: *, $P < 0.05$.

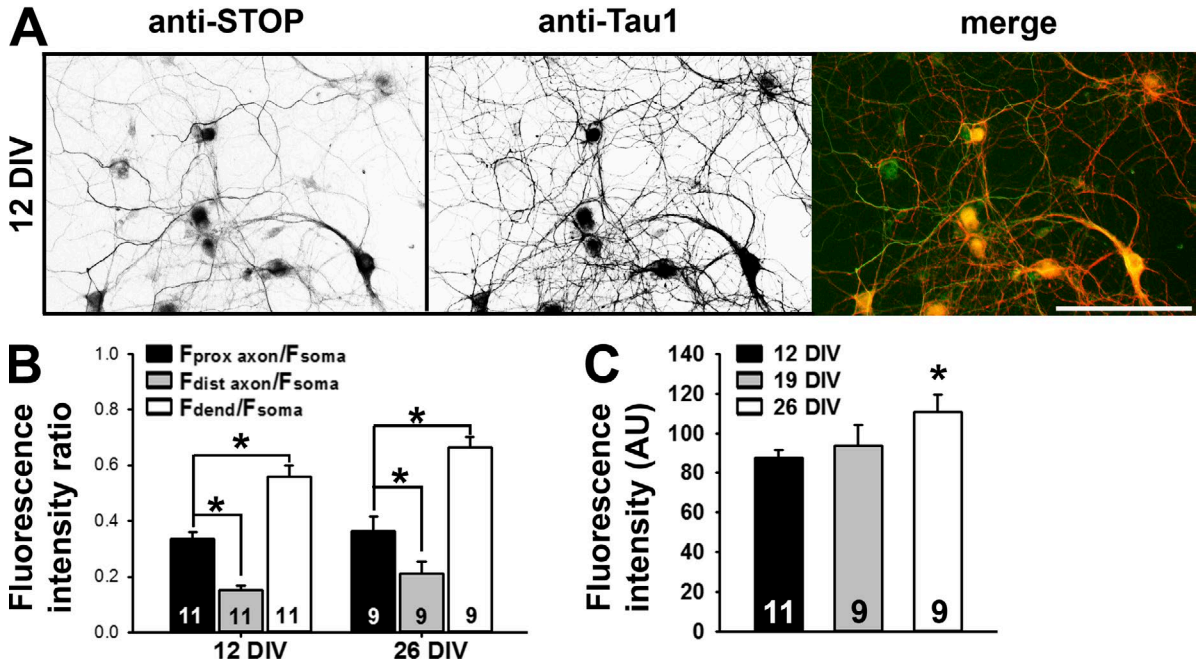

Figure S5. **Development-dependent expression and localization of STOP in cultured hippocampal neurons.** (A) Costaining for endogenous STOP and Tau1 (red in merged). Signals are inverted in grayscale images. Bars, 100 µm. (B) Summary of fluorescence ratios for STOP at different developmental stages. (C) Summary of fluorescence intensities of STOP at the soma at different developmental stages. Error bars indicate means ± SEM. An unpaired *t* test was used in B and a one-way ANOVA followed by Dunnett's test was used in C. *, $P < 0.05$.

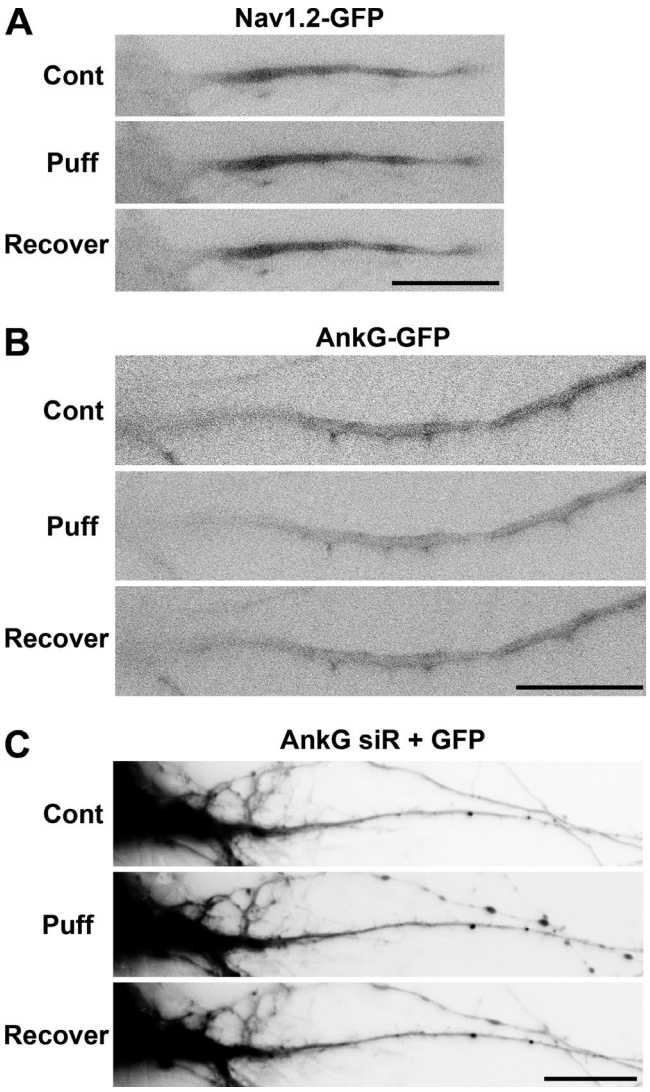

Figure S6. **Alterations of Nav channels and/or AnkG at the AIS do not affect the AIS's resistance to puffing-induced varicosity formation.** (A–C) Puffing with the same procedure as described in Fig. 1 G was performed on the AIS of the neurons transfected with different constructs. (A) The AIS with overexpressed Nav1.2-GFP was still resistant to puffing. Control (Cont), 0 s; Puff, 100 s; Recover, 750 s. GFP signals are inverted. $n = 6$. (B) The AIS with overexpressed AnkG-GFP did not respond to puffing. $n = 7$. (C) The AIS with transfected shRNA against endogenous AnkG (AnkG siR) did not respond to puffing. AnkG siR was previously used and published from our studies to effectively knock down endogenous AnkG and to reduce Nav channel level at the AIS (Xu et al., 2007; Barry et al., 2014). $n = 10$. Bars, 20 µm.

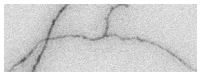

Video 1. **Puffing induced rapid and reversible varicosity formation in axons of young neurons expressing YFP, as shown in the bottom panels of Fig. 1 B.** The interval between frames is 2 s. The total time is 700 s. Signals are inverted.

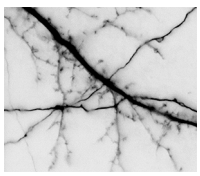

Video 2. **Puffing induced varicosity formation in axons but not in dendrites or dendritic spines of mature neurons expressing YFP, as shown in Fig. 1 F.** The interval between frames is 2 s. The total time is 400 s. Signals are inverted.

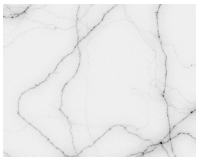

Video 3. **The low magnification view of puffing-induced (by normal Hank's buffer) rapid and reversible varicosity formation in axons of young neurons expressing YFP.** This video is related to Fig. S3 (A–D). The interval between frames is 2 s. The total time is 700 s. Signals are inverted.

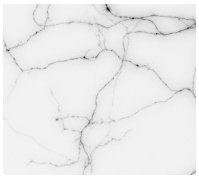

Video 4. **Puffing with the buffer containing no Ca^{2+} and Na^{+} failed to induce varicosities in axons of young neurons expressing YFP.** This video is related to Fig. S3 (A–D). The interval between frames is 2 s. The total time is 700 s. Signals are inverted.

Video 5. **Stimulating NMDA receptors with Glu and Gly induced varicosity formation along dendrites but not axons of mature neurons over time.** This video is related to Fig. 4 (A and B). The interval between frames is 30 s. The total time is 1,800 s. Signals are inverted.

Video 6. **Puffing induced persistent Ca^{2+} increase within varicosities along an axonal segment as shown in Fig. 5 (A and B).** The neuron was loaded with Fluo-4 AM. The interval between frames is 0.5 s. The total time is 90 s.

Video 7. **Puffing induced a transient Ca^{2+} increase in a dendrite as shown in Fig. 5 (F and G).** The neuron was loaded with Fluo-4 AM. The interval between frames is 0.5 s. The total time is 90 s.

References

Barry, J., Y. Gu, P. Jukkola, B. O'Neill, H. Gu, P.J. Mohler, K.T. Rajamani, and C. Gu. 2014. Ankyrin-G directly binds to kinesin-1 to transport voltage-gated Na^{+} channels into axons. *Dev. Cell.* 28:117–131. http://dx.doi.org/10.1016/j.devcel.2013.11.023

Wang, Q., X. Zhang, and Y. Zhao. 2013. Micromechanical stimulator for localized cell loading: fabrication and strain analysis. *J. Micromech. Microeng.* 23:015002. http://dx.doi.org/10.1088/0960-1317/23/1/015002

Xu, M., R. Cao, R. Xiao, M.X. Zhu, and C. Gu. 2007. The axon–dendrite targeting of Kv3 (Shaw) channels is determined by a targeting motif that associates with the T1 domain and ankyrin G. *J. Neurosci.* 27:14158–14170. http://dx.doi.org/10.1523/JNEUROSCI.3675-07.2007